LYCEN - 9366

LYCEN 9366
December 1993

PHENOMENOLOGICAL ANALYSIS OF THE SMALL-x PROTON STRUCTURE FUNCTION $F_2(x, Q^2)$

M. Bertini, P. Desgrolard and M. Giffon
Institut de Physique Nucléaire de Lyon, IN2P3-CNRS
et Université Claude Bernard
F 69622 Villeurbanne Cedex, France

L. Jenkovszky
Institute for Theoretical Physics
Kiev-143, Ukraine

F. Paccanoni
Dipartimento di Fisica, Padova
INFN Sezione di Padova, Italy

Abstract

The recent small-x data on the proton structure function (SF) of the NM, H1 and ZEUS Collaborations are analysed in the framework of various phenomenological parametrizations for the singlet component of the SF. The logarithmic slopes of the SF with respect to $\ell n Q^2$ and $\ell n x$ are calculated and shown as functions of Q^2 and x. Transition regions between different regimes - characteristic of the perturbative and non-perturbative QCD - are discussed.

Submitted to Journal of Physics-G

1. Introduction

The recent publication of the experimental results by the NM [1], H1 [2], and ZEUS [3] Collaborations, opened a new, small-x, area in the study of the proton structure function (SF) $F_2(x, Q^2)$, where maybe for the first time the contributions from the valence quarks (non-singlet SF) can be neglected. This situation, in a way, is reminescent of that in hadronic reactions, where the relative contribution from the secondary reggeons beyond the SPS enery region (i.e. around $\sqrt{s}$ =1 TeV) has become negligible (smaller than the total cross-section error bars).*

The penetration into the small-x region by experimentalists was preceeded and accompanied by an intense theoretical work, concentrated mainly around perturbative QCD calculations of the SF as well as on the estimation of possible shadowing corrections, required by unitarity.

Recently, the small-x behaviour of the SF at small Q^2, outside the perturbative QCD domain, was investigated in [4].

A new and important feature of the small-x data [1-3] is the onset [4,5] of the Pomeron-dominated Regge behaviour (with an apparent logarithmic rise in $x \simeq \frac{Q^2}{s}$ near $Q^2 = 5$ GeV^2), first observed by NMC [1]. An important message from HERA is the acceleration of this rise as Q^2 increases (the increase of the local slope $\frac{d\ell n F_2(x,Q^2)}{d\ell n(1/x)}$ with Q^2). The latter effect, generally speaking, is in agreement with the predictions [6] based on the Gribov-Lipatov-Altarelli-Parisi (GLAP) evolution equation [7], but the range of applicability of these predicitons has not yet been settled. It should be noted that the ZEUS data [3] are below those from H1 [2], however this may be partly attributed to different normalisations. To anticipate the forthcoming presentation, we mention here that the results of the GLAP evolution favour [6] the latter.

We ignore for the time being the valence quark contribution by limiting our analysis to the small-x ($x < 0.1$) region therefore we have not included the large-x data, which, certainly would require the inclusion of non-singlet SF. With the large amount of the experimental data , and the existing theoretical prescriptions available (see e.g.[8]), it would require rather technical work.

In the present paper we first discuss the results of the QCD evolution applied to the small-x HERA data. We then analyse (Secs.3 and 4) the new data by means of several empirical parametrizations inspired both by non-perturbative (Regge) and

---

* This ratio, however, depends on t (moreover, the determination of the real part of the scattering amplitude even at $t = 0$ requires the knowledge of its t-dependence).

In a similar way, in deep inelastic scattering, the x and Q^2-dependence are correlated, and the variation in x of the relative importance of valence quark contribution depends on Q^2 considered.

perturbative QCD (evolution equation) approaches; contrary to Sec.2, we leave the ($\ell n Q^2$)-dependent parameters free and fit them to the data. The small Q^2 limit receives a special treatment in Sec.5.

2. QCD-Analysis of the HERA data

In a recent paper [6], the Q^2-dependence of the proton structure function in the kinematical region of HERA was calculated in a parameter-free way from an input fitted to the NMC data. The result of the evolution was compared to the then available preliminary data of the H1 collaboration. Thereafter, the ZEUS data, covering nearly the same kinematical region were published, offering one more opportunity to test and discuss the results of the theoretical predictions.

We reproduce briefly the arguments and the main results of paper [6]. Its virtue is that the evolution can be calculated analytically with the result given explicitely (see below, Eq.(2)).

The starting point was a Regge-type model for the structure function

$$F_2(x, Q^2) = A\left(1 + \epsilon \ell n(\frac{1}{x})\right), \tag{1}$$

to be evolved in Q^2. The form (1) has been choosen by an observation that the small-x behaviour of the NMC data at $Q^2 = 5$ GeV^2 is the same as that of the hadronic total cross sections at high energies (remember that $x \simeq Q^2/s$ here; for more details see [5]). From this similarity it was conjectured [5] that the singlet SF in the above kinematical region is Regge-behaved and is dominated by a dipole Pomeron contribution. The onset of Regge behaviour (and Pomeron dominance) in the SF is a disputable problem, but the above choice seems to be justified for the following reasons:

1. The kinematical region ($x \sim 10^{-2}, Q^2 = 5$ GeV^2) satisfies the requirements of both: Bjorken scaling (ν and Q^2 large), and Regge behaviour ($\nu >> Q^2$);

2. The "Pomeron" in (1) has the same (and reasonable) intercept $\alpha(0) \approx 1.1$[1,4] as in hadronic reactions.

This, however does not mean that in [5] *the* Regge domain has been found unambiguously. Morever, we are aware that the relation between the Regge behaviour for real and virtual particles is a very delicate problem (see [4] and Sec.5 of the present paper).

In [5], the NMC data have been refitted with the replacement of the "supercritical" Pomeron $x^{\alpha(0)-1}$ by a dipole (1). From the resulting fit the values of ϵ in (1) was found to be $\epsilon = 0.15 \pm 0.05$ [5] , while a (slight) x-dependence of A (neglected in [6]) was found to persist down to lowest x-values.

Starting from the input Eq.(1), in [6] the Q^2-evolution was calculated by means of the GLAP equation with the result

$$F_2(x,\xi) = Ae^{-4.64\xi}\left[x^{-1.44\xi} + \epsilon\, e^{3\xi}\, x^{-0.72\xi}\, \ell n(\frac{1}{x})\right], \tag{2}$$

where

$$\xi = \ell n \frac{\ell n(Q^2/\Lambda^2)}{\ell n(Q_0^2/\Lambda^2)}. \tag{3}$$

In [6] the values $A = 0.3, \epsilon = 0.1, Q_0^2 = 5$ GeV^2 and $\Lambda = 0.2$ GeV were used. Consistency with (1) was provided by the condition that

$$\xi(5\,\mathrm{GeV}^2) = 0. \tag{4}$$

Prediction (2) agrees with the H1 data (see Fig. 1). Note that the $x-$ range of the NMC data does not match that of HERA. To fill the gap, the small-x extrapolation of the "Pomeron" contribution was assumed to be valid at fixed $Q^2 = 5$ GeV^2.

There is very little (practically - no) freedom for any further changes in the calculations within the framework of [6]; the value of Q_0^2 does not affect the results (so, one can set $Q_0^2 = 5$ GeV^2 without any loss of generality), while the corridor resulting from the variation of the QCD scale parameter Λ is negligible.

An important limitation of the approach [6] is the simple form of the large-x behaviour of the SF (remember that the integration in the GLAP equation extends to x=1). The choice of the imput (1) in [6] was based on its link with the Pomeron in hadronic reactions and simplicity that made possible to calculate the evolution analytically.

The results of the evolution, certainly depends on the choice of the input. Better agreement with the data (at the cost of an extra free parameter) is expected with a "supercritical dipole" Pomeron model (see [9] and references therein) to be used instead of (1) (see next section, Fig.4).

In Fig.2 we present also fits of the asymptotic expression resulting from the GLAP evolution equation (see e.g. [8] and references therein)

$$F_2(x,Q^2) = A(Q^2)\exp\sqrt{\frac{16N_c\xi}{b}\ell n(\frac{1}{x})}, \quad b = 11N_c/3 - 2n_f/3 \tag{5}$$

with

$$A(Q^2) = exp(a_0 + a_1\xi + a_2\xi^2)$$

to the HERA data. The values of the fitted parameters are

$$a_0 = -3.25, \quad a_1 = 2.32, \quad a_2 = -4.40.$$

Fig. 2 may indicate that the HERA data are not (yet?) in the regime of the asymptotic (small x) solution of the GLAP equation (the relevant fit with $A(Q^2) = Q^{-2}$ is even worse). Such a conclusion however can be drawn only from an analysis including nonasymptotic terms too (see [8]).

In an attempt to understand better the limitations of various theoretical approaches, we have performed an independent phenomenological analysis of the data, to be presented in the forthcoming sections.

3. Empirical Analysis of the Data

Here we try as far as possible to avoid "theoretical bias" in the analysis of the regularities suggested by the data. To this end, we perform a phenomenological fit of the available small-x data [1-3] with several parametrizations for the singlet component of the proton structure function (we make no difference between the gluon and see quark SF). The x dependence in our formulae

$$F_2(x,Q^2) = e^{a_1(Q^2)}\left[1 + e^{a_2(Q^2)}\,\ell n(\frac{1}{x}) + e^{a_3(Q^2)}\,\ell n^2(\frac{1}{x})\right], \tag{6}$$

$$F_2(x,Q^2) = e^{a_1(Q^2)}\left[1 + e^{a_2(Q^2)}\,\ell n^{a_3(Q^2)}(\frac{1}{x})\right], \tag{7}$$

$$F_2(x,Q^2) = e^{a_1(Q^2)}\left[x^{-a_2(Q^2)} + e^{a_3(Q^2)}x^{-a_4(Q^2)}\,\ell n(\frac{1}{x})\right] \tag{8}$$

is quite general; it is suggested by various combinations of non-perturbative (Regge-type) and perturbative (QCD evolution) approaches (for more details and motivation see below).

Bjorken scaling violation in these expressions enters through the Q^2 dependence of the fitted parameters (see also [10]):

$$a_i(Q^2) = c_{i,0} + c_{i,1}\xi + c_{i,2}\xi^2,$$

where $\xi = \xi(Q^2)$ is the typical perturbative QCD variable given by Eq.(3).

In this way we hope to test various parametrizations for the small-x dependence of F_2, by leaving the Q^2 dependence quite general (polynomial dependence on the "perturbative QCD variable" $\ell n\left[\ell n(Q^2/\Lambda^2)\right]$).

By concentrating on the small-x behaviour only, we neglect the factors of the type $(1-x)^\nu$ responsable for the large-x behaviour of the SF.

Let us now make a few comments on the small-x dependence, as defined by Eqs.(6)-(8) and on the resulting fits, presented by the Fig.3 and Table 1.

Parametrization (6) is obviously an attempt to reproduce the data by a Froissaron-like model, quite successfull in describing hadron diffraction. It fails

however to follow the rapid rise of the slope with Q^2 * .

To clarify this point further, we have fitted the data of [1-3] by Eq.(7). The results are shown in Figs.3.

The "Froissart-like" parametrization (7) does follow the rapid rise seen at HERA but at the cost of a the dramatic increase of the power of the logarithm $a_3(Q^2)$, starting at 2 and reaching 3.5 at $Q^2 = 1000$ GeV^2, (see Fig.4).

The use of (8) gives excellent fits to the data (see Fig.3) and it is another argument favouring the interpretation of the HERA-effect as a manifestation of the Q^2 evolution, in agreement with the perturbative QCD calculations.

Note that there is one exception in the otherwise perfect fit to all of the data from [1-3], namely the data point at $Q^2 = 480$ GeV^2 which is definitely off the overall fits. If further measurements will confirm this data point, it could mean a deviation from a smooth and coherent picture resulting from the above fit.

Quite instructive is Fig.4, where the Q^2-dependence of the powers a_2 and a_4 in Eq.(8) are shown. One can see that the parameter $a_2 \simeq 0.02$ at $Q^2 = 5$ GeV^2, in accord with the condition (4), while the value of $a_4(5 \text{ GeV}^2) = 0.37$ although small, is an indication that the data may prefer a "supercritical" dipole Pomeron as an input instead of (1).

Another interesting feature in the behaviour of the parameters a, as it follows from our fits and is exhibited in Fig.4, is their saturation when Q^2 increases.

Apart from the conventional definition of the slope of the structure function

$$B_1 = \frac{d\ell n F_2(x, Q^2)}{d\ell n Q^2},$$

measuring scaling violation, we introduced also

$$B_2 = -\frac{d\ell n F_2(x, Q^2)}{d\ell n x}$$

as a measure of the deviation from the Froissart bound. They are calculated from Eq.(8), with the parameters fitted to the data and are exibited in Fig. 5 both for fixed x and fixed Q^2. These figures demonstrate once more the violent rise of F_2 both in x and in Q^2 (the HERA effect).

4. The "NMC-Parametrization" Revisited

The empirical parametrization of the proton structure function [1]

$$F_2(x, Q^2) = x^{a_1} f(x, Q^2), \tag{9}$$

* Another reason why the fitted curve (6) follows the NMC, rather than the HERA data is the large number of the data points and the relative smallnes of the error bars of NMC.

where

$$f(x,Q^2) = A(x)\left[\frac{\ell n(Q^2/\Lambda^2)}{\ell n(Q_0^2/\Lambda^2)}\right]^{B(x)}\left[\frac{1+C(x)}{Q^2}\right],$$

$$Q_0 = 20\ \mathrm{GeV}^2\,, \quad \Lambda = 250\ \mathrm{MeV}$$

$$A(x) = (1-x)^{a_2}\left[a_3 + a_4(1-x) + a_5(1-x)^2 + a_6(1-x)^3 + a_7(1-x)^4\right],$$

$$B(x) = b_1 + b_2 x + \frac{b_3}{(x+b_4)}\,, \quad C(x) = c_1 x + c_2 x^2 + c_3 x^3 + c_4 x^4$$

was successfull in fitting the NMC data and it served in [5] as a basic argument supporting the Pomeron dominance in that region.

This parametrization was originally intented to cover the kinematical range of NMC, BCDMS and SLAC data (for relevant references, see [1]). Nevertheless, it is of a certain interest to refit (9) with the HERA data points included, using the same $x = 0.1$ upper limit as we did throughout this work.

The results are shown in Fig.6 with the values of the fitted parameters presented in Table 2. The agreement with the data is quite good.

It is interesting to note that the parameter $-a_1$=("Pomeron intercept"*-1) in Eq.(9) assumes the value 0.28 (instead of 0.101 in [1]).

Since the Pomeron intercept should be Q^2-independent**, the increasing value of $|a_1|$ in Eq.(9) mimics the power behaviour, required by Q^2 evolution, as argued in [6] (see also the reference [7] in that paper). For this reason, any conclusion - even though numerically consistent - that the HERA results confirm (or approach to) the "Lipatov hard Pomeron" (for the derivation - but not applicability! - of this Pomeron see e.g. [11] and earlier references therein) is conceptually superficious. What remains yet to be settled are the details of the transition from one (e.g. Regge) regime to another one (LLA, DLA approximations of the perturbative QCD and possible non-perturbative corrections due to saturation in the partonic density etc.).

Attempting to clarify this point, and searching for further links between the behaviour of the hadronic reactions and the deep inelastic scattering, in the spirit of [5] ,we have replaced the "supercritical Pomeron" x^{a_1} in (9) by a logarithmic expansion:

$$F_2(x,Q^2) = \left(1 + \epsilon_1\,\ell n(\frac{1}{x}) + \epsilon_2\,\ell n^2(\frac{1}{x})\right) f(x,Q^2), \tag{10}$$

---

* The quotation mark indicates that the standard notion of the Pomeron (and its intercept) cannot be used here since at HERA (typically $Q^2 \sim 10^2$ GeV^2), the condition $Q^2 << \nu$ is not safe any more.

** Regge behaviour, and the Pomeron intercept, in particular, do not depend on the masses or virtualities of the external particles.

where the logarithms at small Q^2 may be interpreted (with the above reservation) as a series of multipole Pomerons.

The resulting fits are shown in Fig.6 in comparison with the fits of the preceeding formula (9); the values of the fitted parameters are quoted in Table 2. Contrary to the case of parametrization (6), here the logarithms in $\frac{1}{x}$ do follow the rise of F_2 from NMC to HERA.

Notably, the parameters ϵ_1, ϵ_2 from the present fit differ form those obtaind from relevant fits to hadron-hadron reactions [9]. However this is understandable as explained above.

5. Small-Q^2 limit of the SF

The small-Q^2 region is definitively outside the range of the perturbative QCD. Little is known about this region, apart from the requirement imposed by gauge invariance that F_2 should vanish linearly with Q^2 as Q^2 tends to zero. The parametrizations discussed above are inapplicable in the small Q^2-limit and they do not allow for a smooth transition between the virtual and real photon scattering, for which interesting data have been obtained at HERA [12].

This problem has a long history (see e.g. [13]). A recent treatment can be found in [4], where a smooth transition between the deep inelastic scattering and real photon total cross sections is suggested on the basis of a simple but efficient model for the Pomeron being a simple Regge pole with an intercept slightly above 1 (1.08), such that unitarity practically will be never violated.

Below we propose our version of a (partial) solution of this problem. It is based on the concept of a dipole Pomeron that is selfconsistent from the point of view of the s channel unitarity (for more arguments see [5] and earlier references therein).

Our singlet SF, corresponding to a dipole Pomeron (1), but consistent with the requirement of gauge invariance that it vanishes as $Q^2 \to 0$, has the form

$$F_2(x,Q^2) = A\left[1+\epsilon\,\ell n\left(Q^2(\frac{1}{x}-1)+M^2\right)\right]\ell n\left(1+\frac{Q^2}{Q^2+a^2}\right), \qquad (11)$$

where M is the proton mass and a is an other free parameter (for its physical interpretation see e.g. [4]).

In the limit of $Q^2 \to 0$ we get for the real photon total cross section

$$\sigma_t^{\gamma p} = \frac{4\pi^2\alpha}{Q^2}F_2(x,Q^2). \qquad (12)$$

The resulting fits are shown in Fig.7 with the following values of the fitted parameters:

$$A = 0.475 \quad \epsilon = 0.057 \quad a = 0.713\ \mathrm{GeV}^2.$$

Both solutions - ours and that of [4] - are limited to small values of $Q^2 \sim 5$ GeV^2. The extension of this interpolation to large values of Q^2 is an important but difficult problem for the theorists.

6. Conclusions

To avoid possible uncontrolled effects resulting from the multiple rescattering in the nuclear targets, in the present analysis we have used only data on the proton structure functions, although the available data on nuclear targets (e.g. deuteron [1]) could provide further valuable information on the small-x behaviour of the structure functions.

It is worth noting that apart from the conventional definition of the slope B_1, we have introduced in our analysis the slope B_2 with respect to ℓnx.

The most important lessons from our analysis are:

1. The complicated interplay of the x and Q^2 dependence of the SF is not yet completely understood. Apart form various phenomenological approaches, there are at least two complementary theoretical concepts that may be used as guides: one is the evolution equation and is based on perturbative QCD, the other is the Regge theory. The latter provides us also with a link to the hadronic processes. The most difficult problem remains the applicability (specific kinematical regions) of these approaches or - alternatively - their interface or unifications.

2. Irrespective of the details in the observed small-x behaviour of the SF, the slow-down of their further rise is inevitable as a consequence of the expected saturation of the partonic density. Although this new change of regime is not yet visible in the HERA data, they do not rule it out either.

3. A better account for the large-x domain in the input SF may improve the results of the evolution. The price one has to pay is that the relevant parametrizations do not remain simple any more, and the solution can be found only numerically.

4. The resulting parametrizations can be used as a guide in further studies of the transition effects between perturbative and non-perturbative QCD.

We thank A.Kotikov for usefull discussions. L. J. thanks I.P.N.L. for hospitality and support.

References

1. NM Collab. P. Amaudruz *et al.*, Phys. Lett. B 295 (1992) 159.
2. H1-Collab., I. Abt *et.al.*, Nucl.Phys. B 407 (1993) 515.
3. ZEUS-Collab., M. Derrick *et al.*, Phys. Lett. B 316 (1993) 412.
4. A. Donnachie, P. Landshoff, *Proton Structure Function at Small* Q^2. M/C-TH 93/11 and DAMMTP 93-23 preprint, May 1993.
5. P. Desgrolard, M. Giffon, L.L. Jenkovszky, A.I. Lengyel, E. Predazzi, Phys. Lett. B 309 (1993) 191; see also: L. Jenkovszky, F. Paccanoni, E. Predazzi, Nucl. Phys. B (Proc. Suppl.) B25 (1992).
6. L. Jenkovszky, A. Kotikov, F. Paccanoni, Phys. Lett. B 314 (1993) 421.
7. V.N. Gribov, L.N. Lipatov , Yad. Fiz. 15, (1972) 78 [Sov. J. Nucl. Phys. 15 (1972) 438]; L.N. Lipatov, Yad. Fiz. 20 (1974) 1981; G. Altarelli, G. Parisi, Nucl. Phys. B 126 (1977) 298.
8. Papers from the Workshop on HERA *the New Frontier for QCD*; in Journal of Physics G: Nuclear and Particle Physics, Volume 18, No 10, 1993.
9. P. Desgrolard, M. Giffon, E. Predazzi, *High quality description of elastic high energy data and prediction of new phenomena*, LYCEN 9339, October 1993.
10. J.G. Morfin, Wu-Ki Tung, Z. Phys. C - Particle and Fields 52 (1991) 13.
11. L. N. Lipatov, *Pomeron in QCD and small x deep inelastic scattering*, in "HADRONS-92", Proceedings of the worshop on elastic and diffreative scattering, Kiev, September 1992 and *High-energy asymptotics of multi-colour perturbative QCD* in "HADRONS-93", Proceedings of the worshop on soft physics, Novy Svit, Crimea, May 1993.
12. M. Derrick *et al.* (ZEUS Collab.), Phys. Lett. B 293 (1992) 465; T. Ahmed *et al*, Phys. Lett. B 299 (1992) 374.
13. M. Greco, Nucl. Phys. B63 (1973) 398; H. Abramovich, F.M. Levin, A. Levy, U. Maor, Phys. Lett. B 269 (1991) 465.

	Eq.(6)	Eq.(7)	Eq.(8)
$c_{1,0}$	-1.354	-1.112	-1.114
$c_{1,1}$	-1.515	0.133	-0.218
$c_{1,2}$	-3.139	-0.69	-0.53
$c_{2,0}$	-2.462	-4.626	0.0565
$c_{2,1}$	3.272	-9.99	0.251
$c_{2,2}$	-10.00	-2.765	0.137
$c_{3,0}$	-5.060	2.0	-5.623
$c_{3,1}$	8.935	6.934	-3.527
$c_{3,2}$	-5.352	-2.65	8.188
$c_{4,0}$	–	–	0.366
$c_{4,1}$	–	–	1.473
$c_{4,2}$	–	–	$0.5\,10^{-6}$

Table 1

Values of the parameters obtained from the fits of Eqs.(6)-(8) to the HERA [2,3] and NMC [1] data.

	Eq.(9)	Eq.(10)
	$a_1 = -0.2842$	$\epsilon_2 = 0.28315$
a_2	4.470	3.673
a_3	0.5323	0.2790
a_4	-0.4650	-0.3775
a_5	5.951	6.069
a_6	-10.308	-10.290
a_7	4.441	4.393
b_1	0.3307	0.3325
b_2	-3.478	-3.437
b_3	0.0179	0.0176
b_4	0.0174	0.0169
c_1	-1.927	-1.909

Table 2

Values of the parameters obtained from the fits to the HERA [2,3] and NMC [1] data with the "NMC parametrization" using Eq.(9) and its modification, Eq.(10). We have simplified the parametrization by setting $c_2 = c_3 = c_4 = 0.0$ in both cases and $\epsilon_1 = 0$ in the second case without affecting the resulting fits.

Figure captions

Figure 1. Proton singlet SF, Eq.(2) calculated from the GLAP evolution equation (see text) plotted (a) versus Q^2 and (b) versus x, shown with the small x data. In (b), the NMC data [1] are shown at $Q^2 = 5$ GeV^2, while higher Q^2 data correspond to H1 [2] (hollow triangles) and ZEUS [3] (full dots).

Figure 2. Asymptotic solution Eq.(5) of the GLAP equation confronted to the HERA data.

Figure 3. Fits to the small-x data of the phenomenological parametrizations of Sec.3; dashed, dotted and solid lines correspond to Eqs.(6), (7), (8), respectively. In figs. (a) and (b) hollow triangles correspond to the H1 data [2], and full dots to the ZEUS data [3]. The values of the fitted parameters are quoted in Table 1.

Figure 4. Q^2 dependence of the powers a_2 and a_4 in Eq.(8).

Figure 5. Logarithmic slopes $B_1 = \frac{d\ell n F_2(x,Q^2)}{d\ell n Q^2}$ (top of the figure) and $B_2 = -\frac{d\ell n F_2(x,Q^2)}{d\ell n x}$ (bottom of the figure), as functions of x and Q^2 calculated from Eq.(8)

Figure 6. Fits of Eq.(9) to the data with a "supercritical Pomeron" (solid line) and of Eq.(10) with "multipole pomerons" (dashed line): (a,b) SF versus x, (b,c) SF versus Q^2. In (a) and (b) hollow triangles correspond to the H1 data [2], and full dots to the ZEUS data [3].

Figure 7. Small-Q^2 fits to the SF Eq.(11).

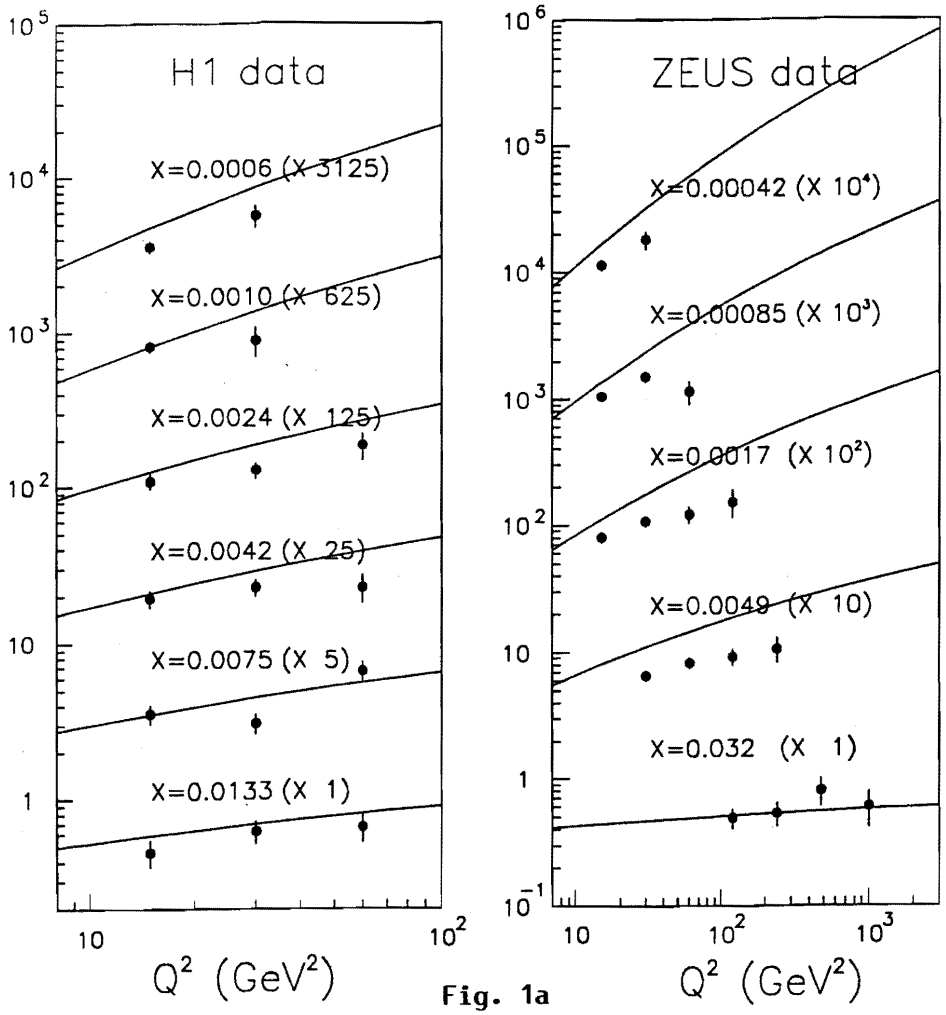
H1 data
X=0.0006 (X 3125)
X=0.0010 (X 625)
X=0.0024 (X 125)
X=0.0042 (X 25)
X=0.0075 (X 5)
X=0.0133 (X 1)
Q² (GeV²)
ZEUS data
X=0.00042 (X 10⁴)
X=0.00085 (X 10³)
X=0.0017 (X 10²)
X=0.0049 (X 10)
X=0.032 (X 1)
Q² (GeV²)

Fig. 1a

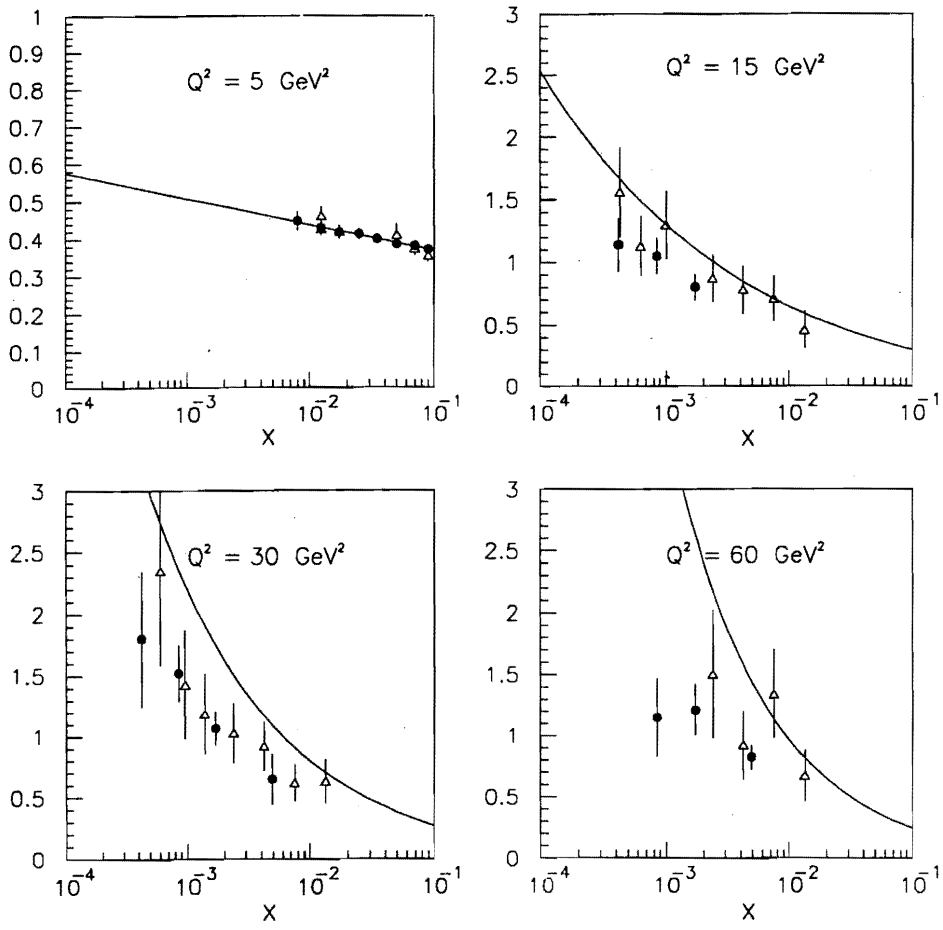
Q² = 5 GeV²
Q² = 15 GeV²
Q² = 30 GeV²
Q² = 60 GeV²
X

Fig. 1b

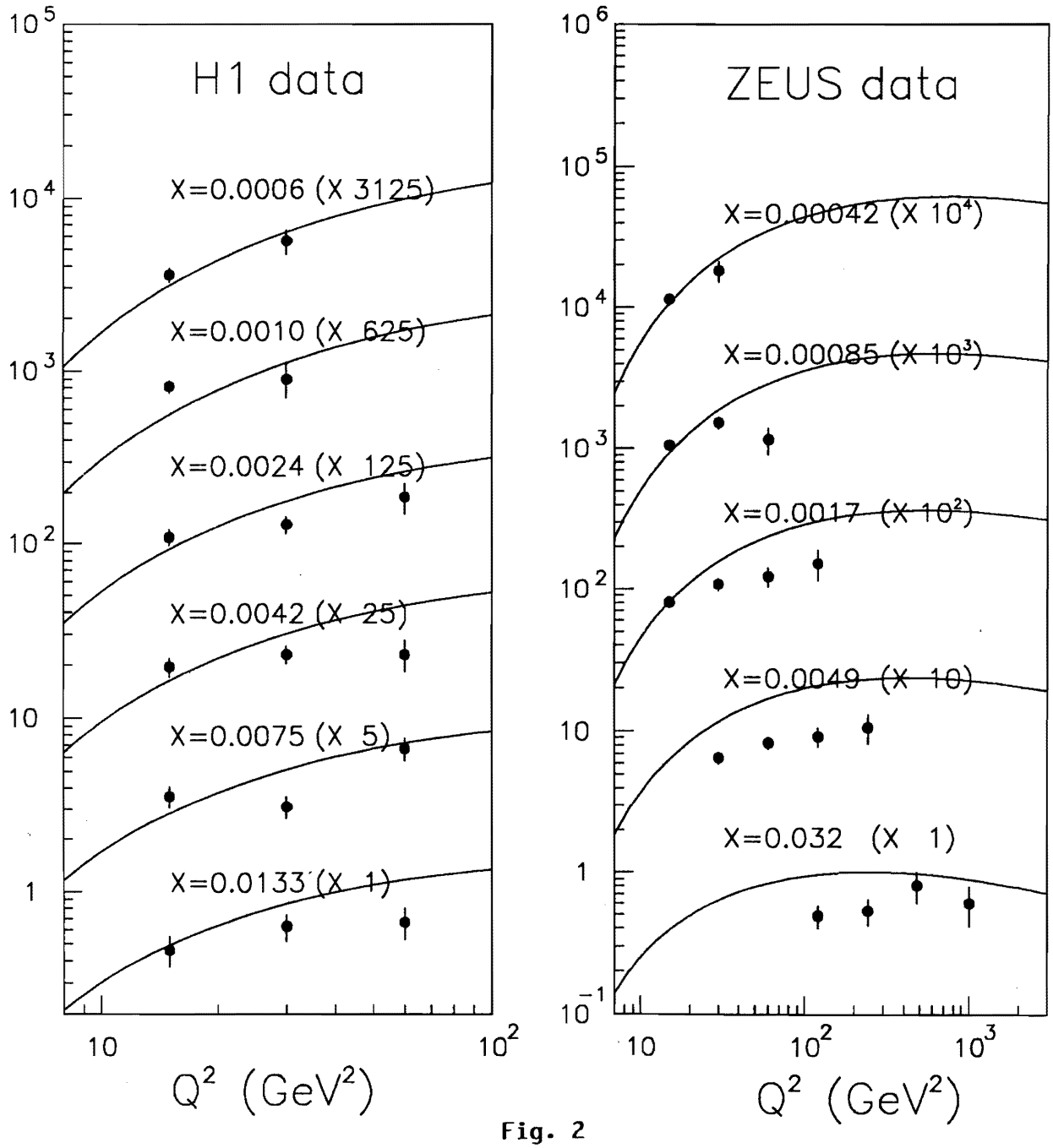
H1 data
X=0.0006 (X 3125)
X=0.0010 (X 625)
X=0.0024 (X 125)
X=0.0042 (X 25)
X=0.0075 (X 5)
X=0.0133 (X 1)
10^5
10^4
10^3
10^2
10
1
10
10^2
Q^2 (GeV^2)
ZEUS data
X=0.00042 (X 10^4)
X=0.00085 (X 10^3)
X=0.0017 (X 10^2)
X=0.0049 (X 10)
X=0.032 (X 1)
10^6
10^5
10^4
10^3
10^2
10
1
10^{-1}
10
10^2
10^3
Q^2 (GeV^2)

Fig. 2

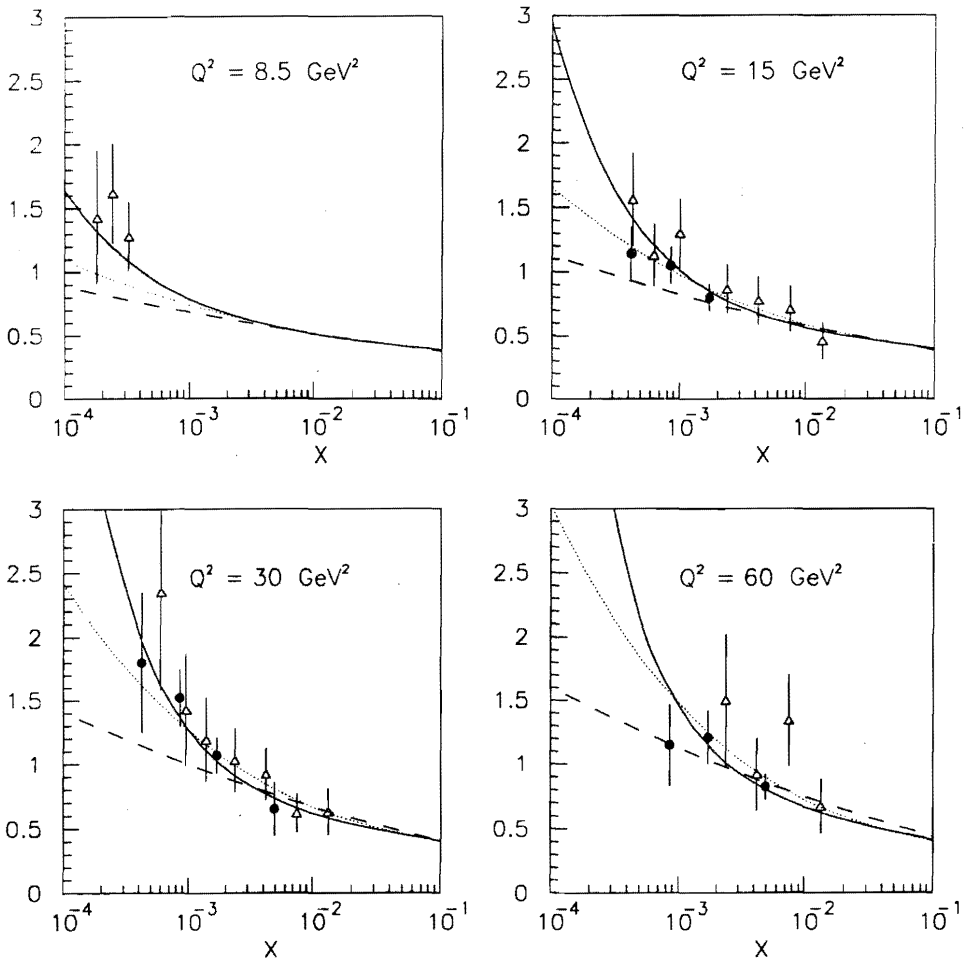
Q² = 8.5 GeV²
Q² = 15 GeV²
Q² = 30 GeV²
Q² = 60 GeV²
X

Fig. 3a

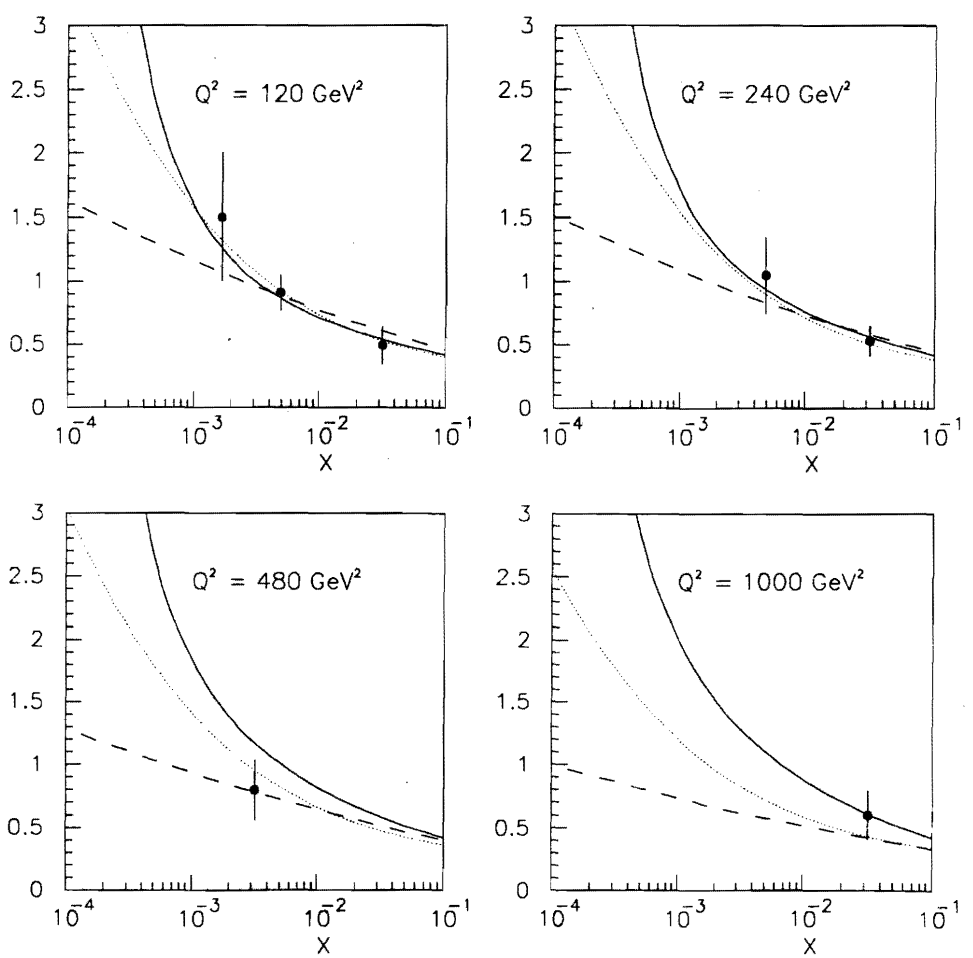
Q² = 120 GeV²
Q² = 240 GeV²
Q² = 480 GeV²
Q² = 1000 GeV²
X

Fig. 3b

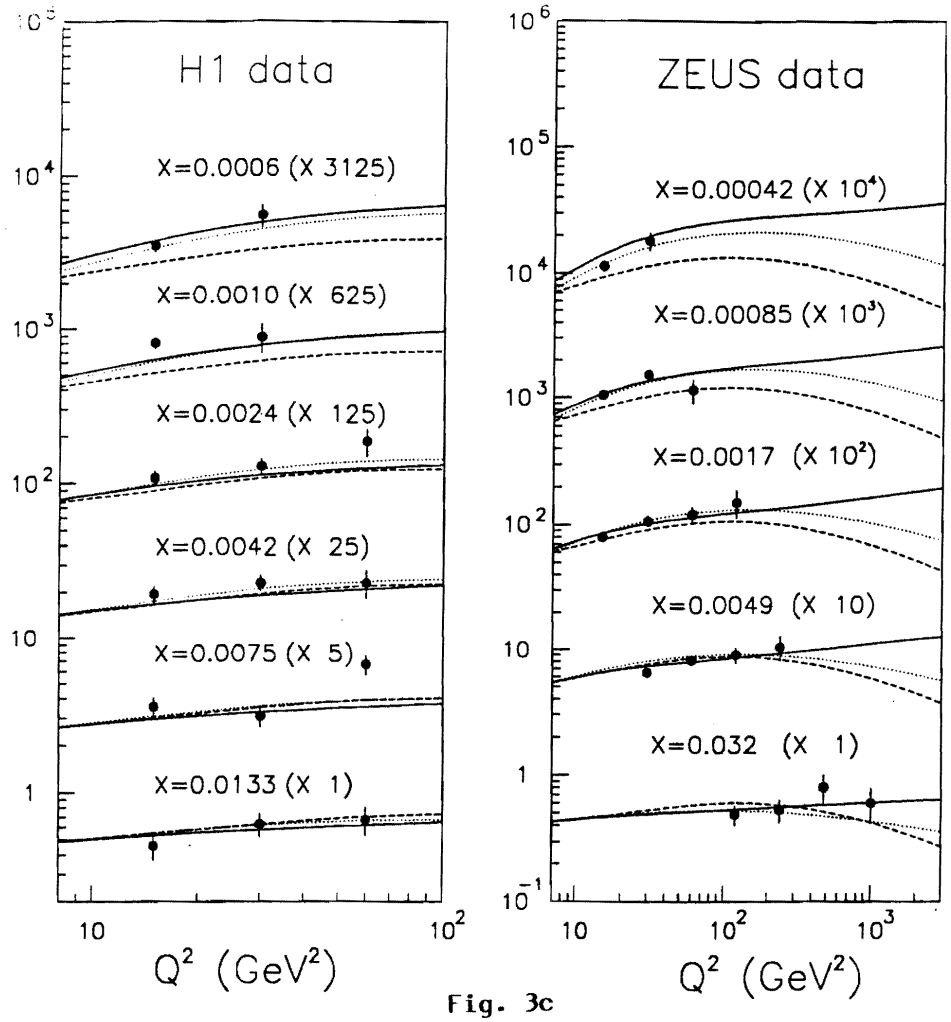
H1 data
X=0.0006 (X 3125)
X=0.0010 (X 625)
X=0.0024 (X 125)
X=0.0042 (X 25)
X=0.0075 (X 5)
X=0.0133 (X 1)
ZEUS data
X=0.00042 (X 10^4)
X=0.00085 (X 10^3)
X=0.0017 (X 10^2)
X=0.0049 (X 10)
X=0.032 (X 1)
Q^2 (GeV^2)
Q^2 (GeV^2)

Fig. 3c

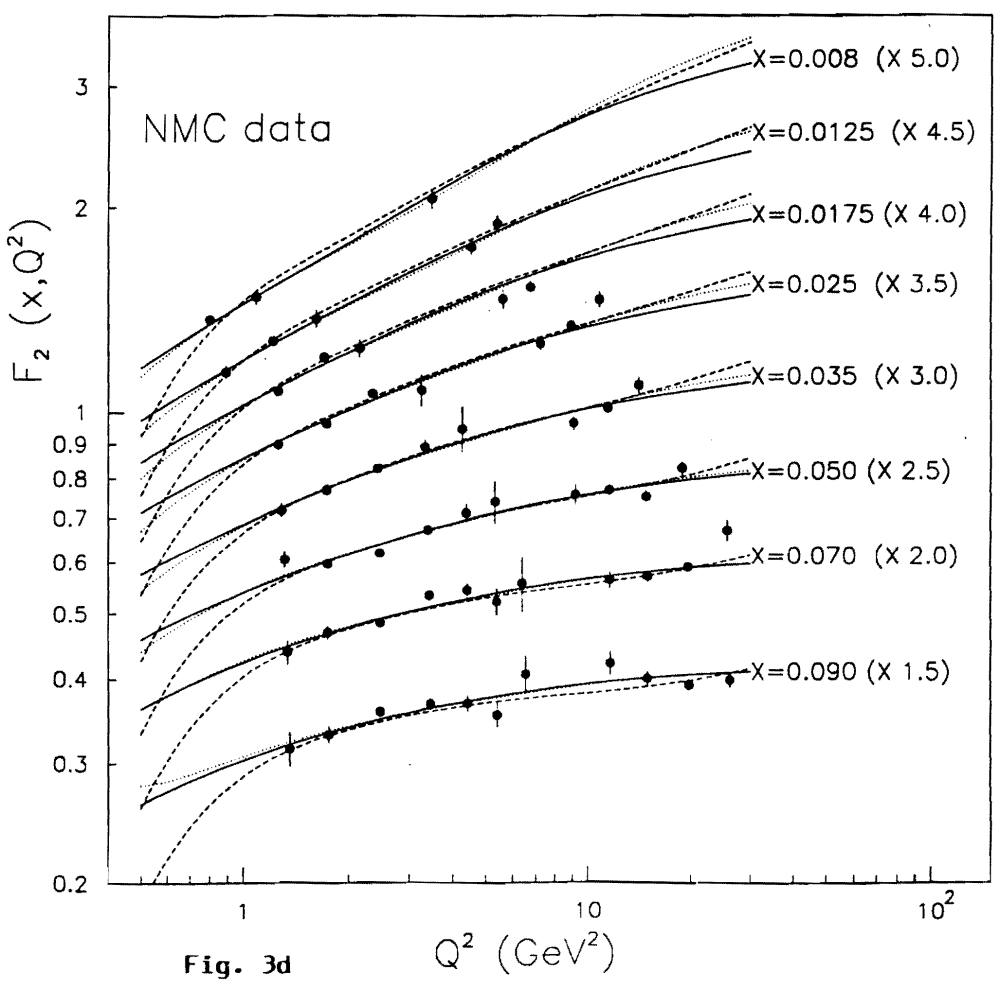
NMC data
X=0.008 (X 5.0)
X=0.0125 (X 4.5)
X=0.0175 (X 4.0)
X=0.025 (X 3.5)
X=0.035 (X 3.0)
X=0.050 (X 2.5)
X=0.070 (X 2.0)
X=0.090 (X 1.5)
F_2 (x,Q^2)
Q^2 (GeV^2)

Fig. 3d

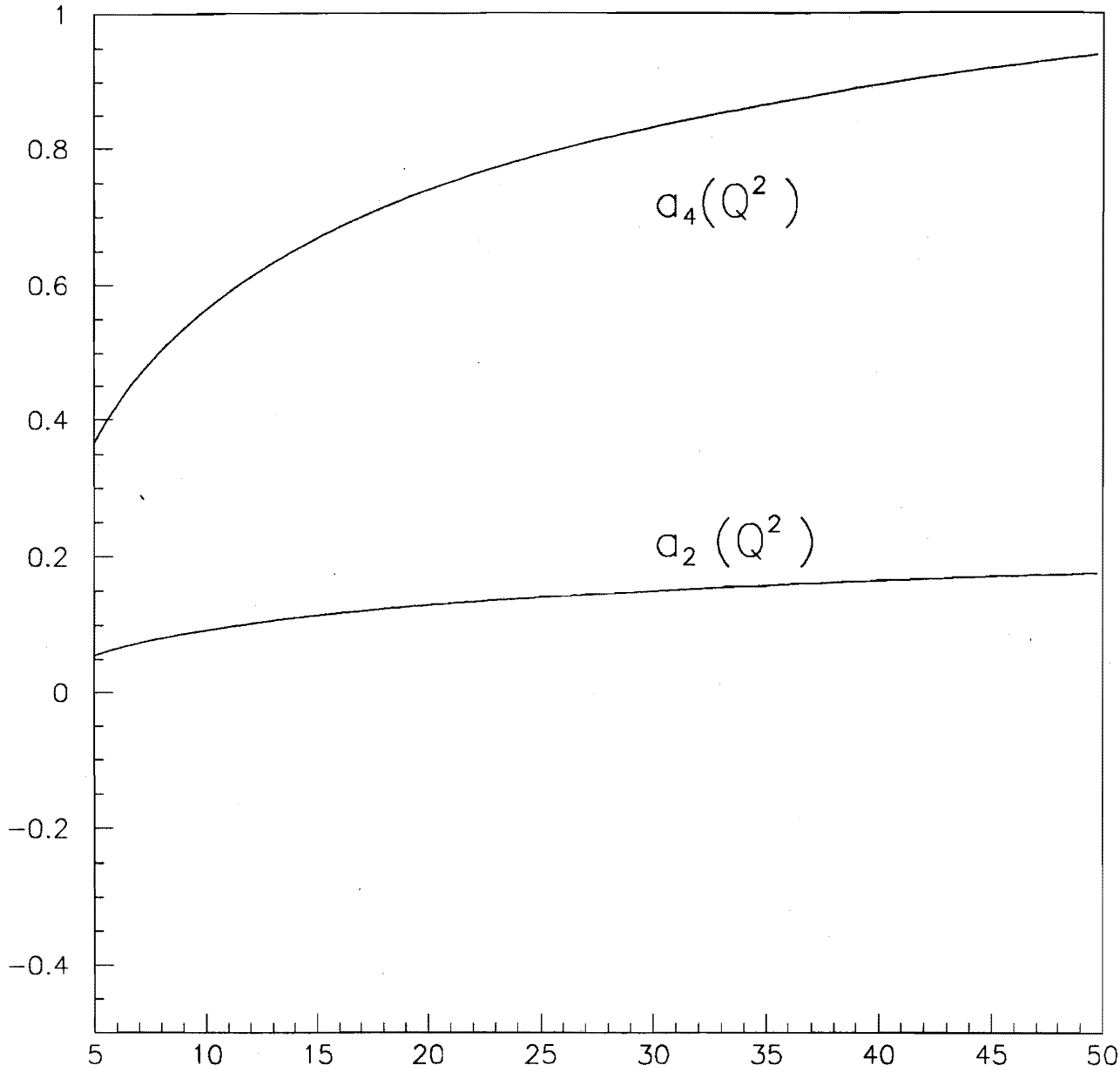

Fig. 4

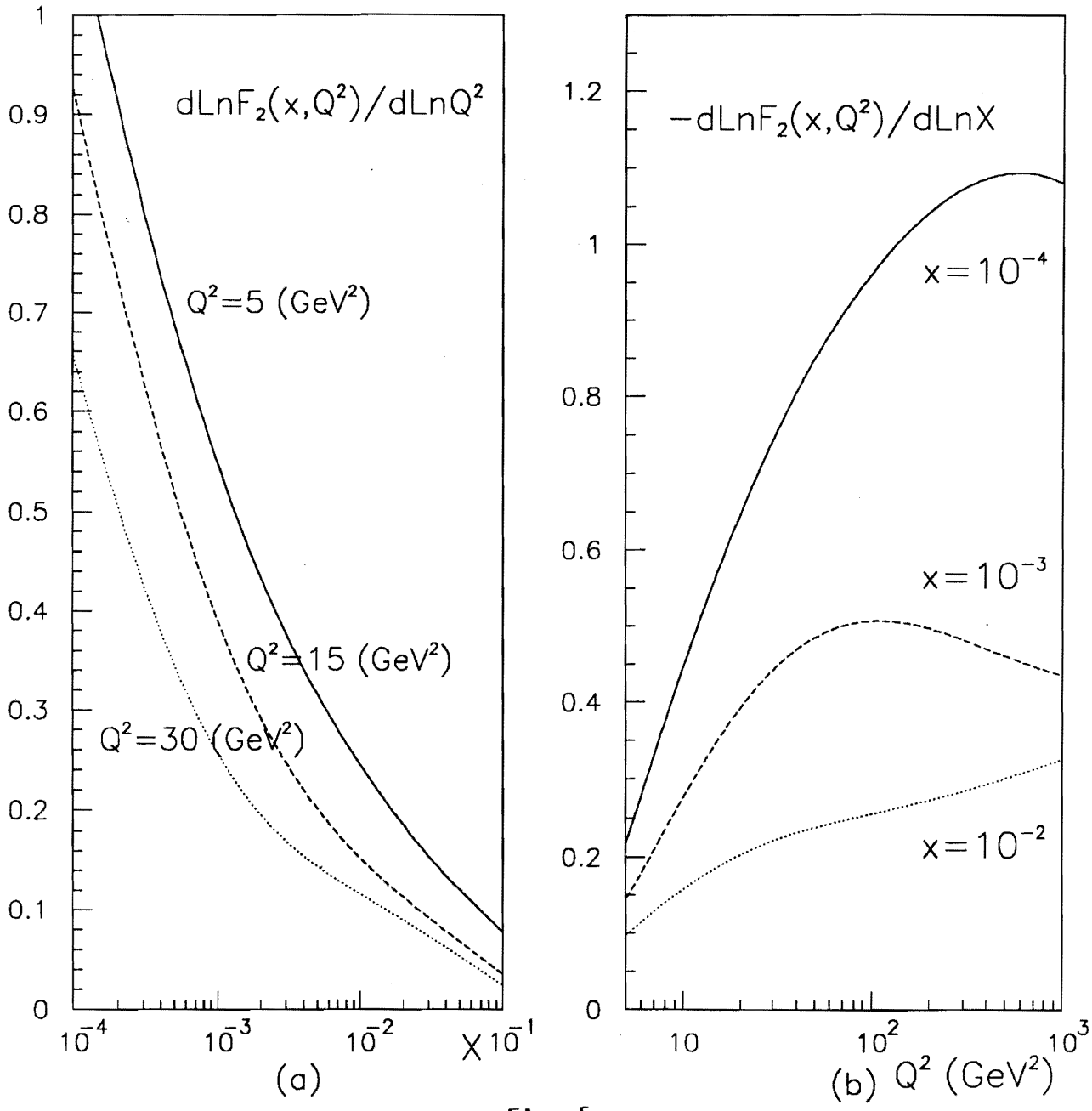
dLnF2(x,Q2)/dLnQ2
Q2=5 (GeV2)
Q2=15 (GeV2)
Q2=30 (GeV2)
X
(a)
−dLnF2(x,Q2)/dLnX
x=10−4
x=10−3
x=10−2
Q2 (GeV2)
(b)

Fig. 5

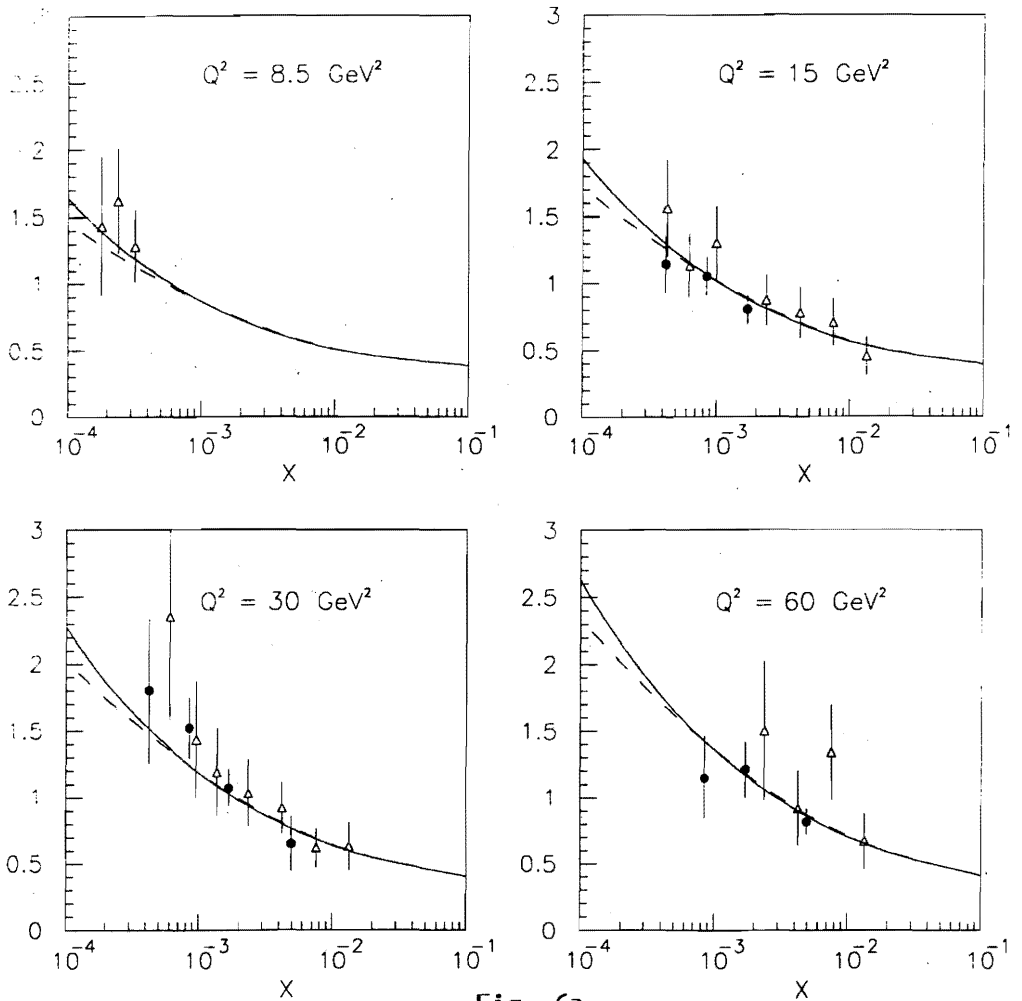
Q² = 8.5 GeV²
Q² = 15 GeV²
Q² = 30 GeV²
Q² = 60 GeV²
X

Fig. 6a

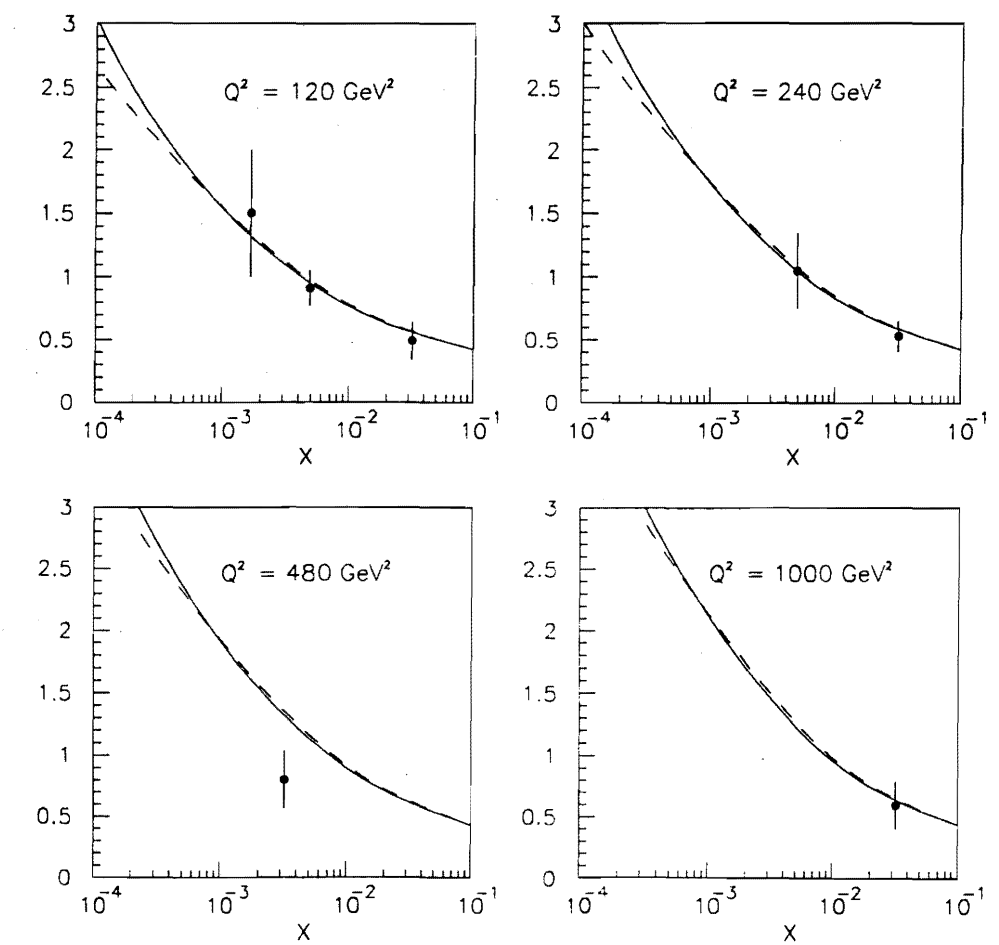
Q² = 120 GeV²
Q² = 240 GeV²
Q² = 480 GeV²
Q² = 1000 GeV²
X

Fig. 6b

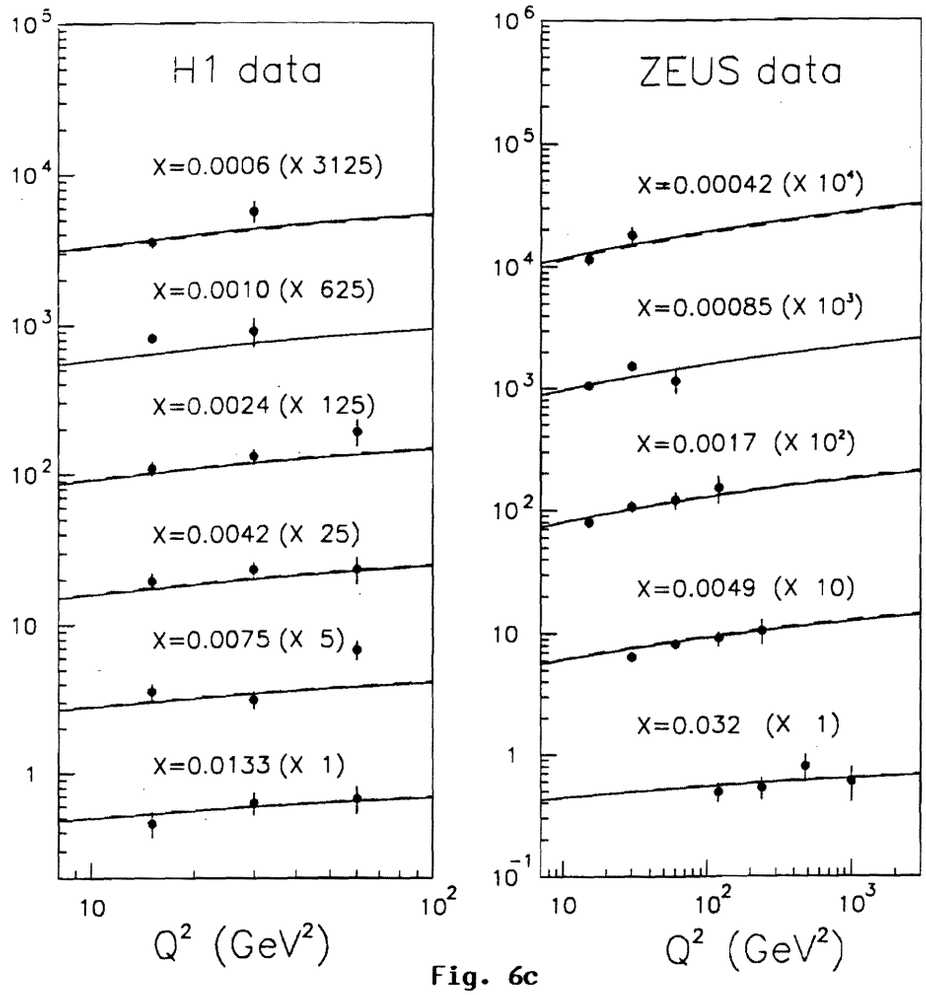
H1 data
X=0.0006 (X 3125)
X=0.0010 (X 625)
X=0.0024 (X 125)
X=0.0042 (X 25)
X=0.0075 (X 5)
X=0.0133 (X 1)
ZEUS data
X=0.00042 (X 10⁴)
X=0.00085 (X 10³)
X=0.0017 (X 10²)
X=0.0049 (X 10)
X=0.032 (X 1)
Q² (GeV²)
Q² (GeV²)

Fig. 6c

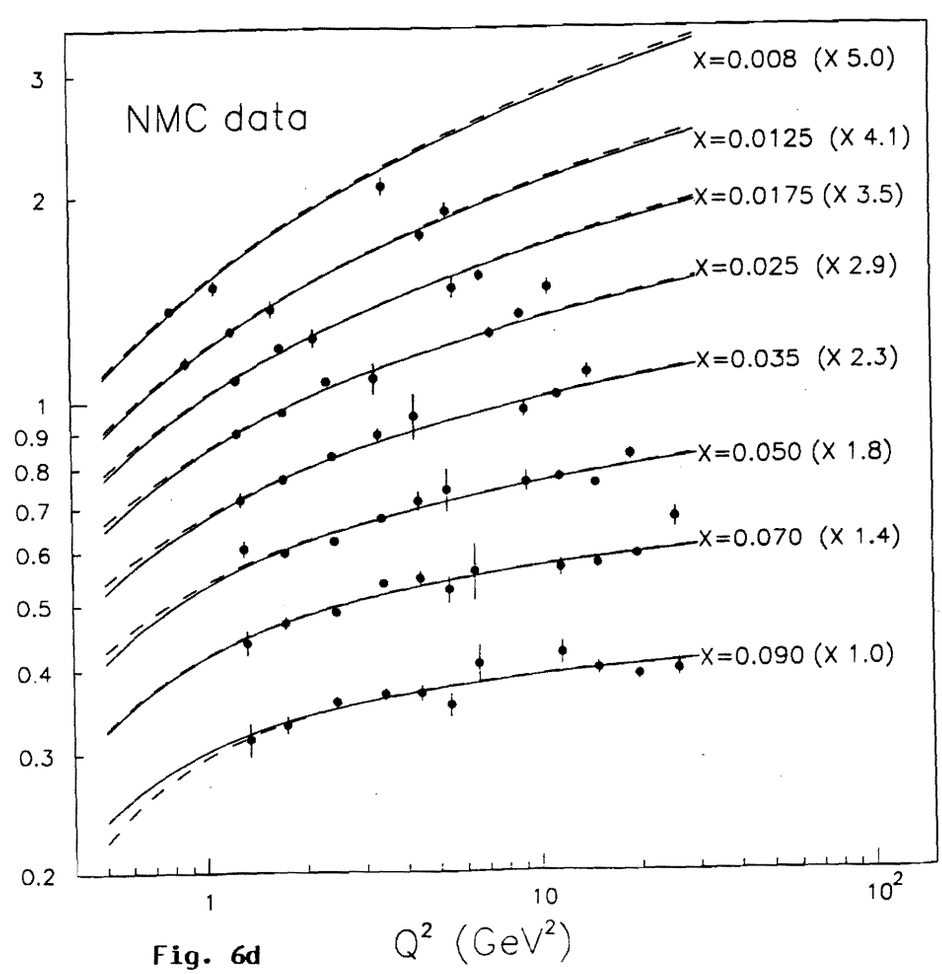
NMC data
X=0.008 (X 5.0)
X=0.0125 (X 4.1)
X=0.0175 (X 3.5)
X=0.025 (X 2.9)
X=0.035 (X 2.3)
X=0.050 (X 1.8)
X=0.070 (X 1.4)
X=0.090 (X 1.0)
Q² (GeV²)

Fig. 6d

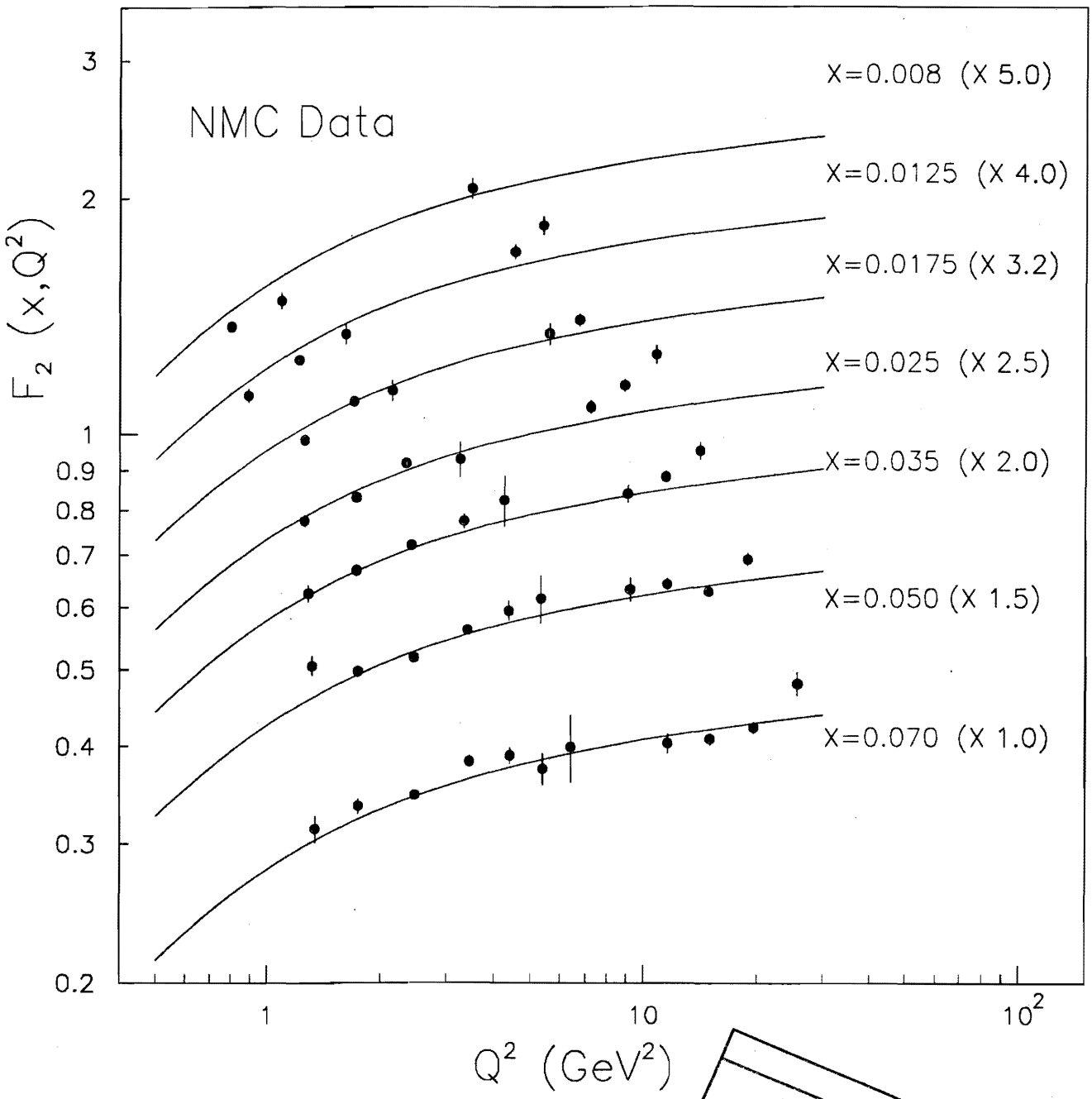

Fig. 7

NAME
I.D.No
M.S.